Contents

Chapter 1

Introduction

Chapter 2

Multi-armed bandits

The multi-armed bandit (MAB) problem is a classic problem in reinforcement learning and probability theory. It poses a simple yet challenging problem, where the agent must sequentially choose between a number of arms (distributions) of which the mean reward is unknown, trying to maximise the cumulative reward. This poses a constant struggle between exploration and exploitation, where exploration is the process of trying out new arms, and exploitation is the process of sampling from the distribution with the highest average thus far.

Although the bandit term was not coined before 1952 [1], its study dates back to 1933 [2]. The problem of choosing between two treatments for patients was considered: to what degree should the most successful treatment be used versus testing the other to ensure that the truly best is indeed used?

Some of the many real-world setting where the multi-armed bandit problem is applicable are listed in table 2.1. Despite being a simple problem, its countless variants and applications make it not only a useful tool for real-world problems. Netflix uses MAB theory to recommend movies [3], Amazon for its website layout [4], Facebook for video compression [5] and Doordash to identify responsive deliverymen [6]. The problem and its variations are still being studied with several results in what follows being recent.

This chapter and its notation will mostly follow the work textbook [7], to which the interested reader is referred for more details on the bandit problem and its variants.

Table 2.1: Some applications of the multi-armed bandit problem.

Application	Arms	Reward
Medical trials	Drugs	Patient health
Online advertising	Ad placements	Number of clicks
Website design	Layouts/fonts &c.	Number of clicks
Recommendation systems	Items	Number of clicks
Dynamic pricing	Prices	Profit
Networking	Routes, settings	Ping
Lossy compression	Compression settings	Quality preserved
Tasking employees	Which employee	Productivity
Finance	Investment options	Profit

2.1 Problem definition

In the multi-armed bandit problem the agent has knowledge of the set of available actions $\mathcal{A} = \{1, \ldots, k\}$, but not the reward distributions $\nu = \{P_a : a \in \mathcal{A}\}$. For each time step $t = 1, \ldots, T$, the agent selects an action $a_t \in \mathcal{A}$ and receives a reward $X_t \sim P_{a_t}$, independent of previous samples. The time horizon T is usually finite and given, but for many applications, knowledge of it unreasonable, motivating the need for anytime algorithms. Nonetheless, it will be assumed greater than k, such that all arms may be pulled. The goal of the agent is to maximise its cumulative rewards.

2.1.1 Assumptions

With no assumptions on the reward distributions, analysis is difficult. It is therefore common to make some assumptions on the reward distributions, defining bandit classes

$$\mathcal{E} = \{\nu = \{P_a : a \in \mathcal{A}\} : P_a \text{ satisfies some property } \forall a \in \mathcal{A}\}. \quad (2.1)$$

Some common bandit classes are listed in table 2.2. Note than some classes are parametric, like Bernoulli and Gaussian bandits, while others are non-parametric, such as the sub-Gaussian and bounded value bandits. Only cases void of any inter-arm structure are considered; knowledge of the mean of one arm should never be used to infer the mean of another.

Table 2.2: Common bandit classes.

Class	Symbol	Definition
Bernoulli	$\mathcal{E}_{\mathrm{B}}^{k}$	$X_a \sim \mathrm{B}(\mu_a)$
Gaussian, unit variance	$\mathcal{E}_{\mathrm{N}}^{k}(1)$	$X_a \sim \mathrm{N}(\mu_a, 1)$
Gaussian, known variance	$\mathcal{E}_{\mathrm{N}}^{k}(\sigma^2)$	$X_a \sim \mathrm{N}(\mu_a, \sigma^2)$
Gaussian, unknown variance	$\mathcal{E}_{\mathrm{N}}^{k}$	$X_a \sim \mathrm{N}(\mu_a, \sigma_a^2)$
Sub-Gaussian	$\mathcal{E}_{\mathrm{SG}}^{k}(\sigma^2)$	$P(|X_a| \geq \epsilon) \leq 2e^{-\epsilon^2/\sigma^2}$
Bounded value	$\mathcal{E}_{[0,1]}^{k}$	$X_a \in [0,1]$
Bounded maximum	$\mathcal{E}_{(-\infty,b]}^{k}$	$X_a \leq b$
Bounded variance	$\mathcal{E}_{\mathrm{Var}}^{k}(\sigma^2)$	$\mathrm{Var}(X_a) \leq \sigma^2$
Bounded kurtosis	$\mathcal{E}_{\mathrm{Kurt}}^{k}(\kappa)$	$\mathrm{Kurt}(X_a) \leq \kappa$

It is assumed to be only one optimal arm, which is the arm with the highest mean reward.

2.1.2 Policies

When interacting with the environment, the agent must select an action at each time step. Hence, a history,

$$\mathcal{D} = \{A_1, X_1, \ldots, A_t, X_t\}, \tag{2.2}$$

is formed, where A_t is the action taken at time t and X_t is the reward received according to the distribution P_{A_t}. The policy $\pi = (\pi_t)_{t=1}^{T}$ is a sequence of probability distributions over the set of actions $\mathcal{A}$. At each time step t, the agent selects an action $a_t \sim \pi_t \mid \mathcal{D}$. To define an algorithm, a policy

$$\pi_t(a \mid A_1, X_1, \ldots, A_{t-1}, X_{t-1}) = \pi_t(a \mid \mathcal{D}) \tag{2.3}$$

is needed for each time step t, from which samples can be drawn.

2.1.3 Regret

For the analysis of algorithm performance, the regret is used. Given a bandit instance nu and a policy π, at round T, the regret is defined as

$$R_T(\pi, \nu) = \mathbb{E}_{\pi,\nu} \left[\sum_{t=1}^{T} \mu^* - X_t \right], \tag{2.4}$$

where μ^* is the highest mean reward and the expectation is taken over both the reward distributions and the potentially probabilistic policy. Often the dependence on particular instances and policies are irrelevant or clear from the context and are therefore omitted.

The usage of regret over the sum of rewards provides several advantages. Firstly, it serves as a normalised measure of performance, wherein perfect performance is achieved when the regret is zero. Secondly, it permits the usage of asymptotic notation for the analysis of algorithm performance as a function of the time horizon T. Finally, considering expectation rather than the stochastic sum of rewards makes the optimisation problem well-defined without having to introduce any utility measure or other assumptions.

It may be more convenient to express the regret in terms of the number of times each action has been selected, irrespective of time. Letting T_a be the number of times action a has been selected up to time T, and using the finitude of $\mathcal{A}$ and linearity of expectations, the regret can be rewritten as

$$R_T = \sum_{a \in \mathcal{A}} \Delta_a \mathbb{E}[T_a], \tag{2.5}$$

where $\Delta_a = \mu^* - \mu_a$ is what is known as the suboptimality gap of action a.

2.2 Variants

2.2.1 Best-arm identification

An alternative problem is to find the best arm with as few turns as possible. In this version, a δ is given, and the goal is to find the best arm with probability at least $1 - \delta$. The metric here is how the turns needed grows as a function of δ. Unlike regret minimisation, exploitation is less of a concern, but much theory can be transferred from the regret minimisation problem. Though there is no direct benefit from exploitation, as there is in regret optimisation, it is still desirable to mainly pull good arms, as these will need more consideration to be distinguished from the best.

2.2.2 Bandit generalisations

The multi-armed bandit problem has numerous generalisations, including the non-stationary multi-armed bandit where the underlying reward distributions change over time, presenting a challenging environment for traditional algorithms developed for the standard, stationary multi-armed bandit problem. In this variant, agents must continuously explore and adapt

to the changing environment. Other cases give the agent more info, such as letting it know what the rewards for all arms, were they pulled instead, would have been. Another area of study is the contextual multi-armed bandit problem, in which contextual information must be incorporated into the decision-making process for arm selection, adding a layer of complexity to the standard multi-armed bandit problem, particularly useful for recommender systems, where the context is the user and their preferences. Moreover, the adversarial multi-armed bandit problem represents a significant departure from the standard, stochastic multi-armed bandit problem, where rewards are chosen by an adversary instead of following a stationary distribution. The infinite-armed variants, where the arm space is infinite but constrained by for example linearity, also have practical applications. While beyond the scope of this report, these generalisations of the multi-armed bandit problem represent important areas of study and much of the theory developed for the standard, stochastic multi-armed bandit problem can be extended to these problems as well [8, 7].

2.3   Optimality

In the realm of multi-armed banditry, expressing optimality is fraught with difficulties. Any precise formulation is contingent upon not only the assumptions made, but also the particular instance, namely actual means and any other parameters. No distributions are placed on the bandit classes $\mathcal{E}$, so no average regret over all instances can be defined. Lower bounds resort then to either determine what a reasonable policy can achieve on a given instance, or to describing its worst performance over all instances in the class.

2.3.1   Instance-dependent lower bound

In order to meaningfully define a lower bound, it is imperative to assume a reasonable algorithm. Otherwise, trivial policies, such as always pulling the first arm, could achieve zero regret, hindering any meaningful comparison. A useful assumption is that the algorithm is asymptotically consistent in some class $\mathcal{E}$, which by definition means that for all inferior arms and all $\eta \in (0, 1)$, it holds that

$$\mathbb{E}[T_a] = o(T^\eta), \tag{2.6}$$

for all instances $\nu \in \mathcal{E}$.

For asymptotically consistent and bandit classes with reward distributions parametrised by only one parameter, the Lai-Robbins bound [9] holds.

It states that

$$\liminf_{T\to\infty} \frac{\mathbb{E}[T_a]}{\ln T} \geq \frac{1}{D(P_a \parallel P^*)}, \tag{2.7}$$

where P_a is the reward distribution of arm a, P^* that of the optimal distribution and $D(\cdot \parallel \cdot)$ the Kullback-Leibler divergence. The Kullback-Leibler divergence is a measure of the difference between two probability distributions over the same space $\mathcal{X}$, defined as

$$D(P \parallel Q) = \sum_{x \in \mathcal{X}} P(x) \log \frac{P(x)}{Q(x)} \tag{2.8}$$

for discrete distributions and

$$D(P \parallel Q) = \int_{\mathcal{X}} P(x) \log \frac{P(x)}{Q(x)} \, dx \tag{2.9}$$

in the continuous case. For more general bandit classes, given finite means, the Kullback-Leibler in the denominator of eq. (2.10) is instead taken to the distribution in that class which is closest to P_a and with mean equal to the mean of P^*,

$$\liminf_{T\to\infty} \frac{\mathbb{E}[T_a]}{\ln T} \geq \frac{1}{d(P_a, \mu^*, \mathcal{E})}, \tag{2.10}$$

where

$$d(P_a, \mu^*, \mathcal{E}) = \inf_{P \in \nu \in \mathcal{E} \text{ for some } \nu} \left\{ D(P_a \parallel P) : \mathbb{E}[P_a] > \mu^* \right\}. \tag{2.11}$$

From eq. (2.5), it follows that

$$\liminf_{T\to\infty} \frac{R_T}{\ln T} \geq \sum_{a \in \mathcal{A}} \frac{\Delta_a}{d(P_a, \mu^*, \mathcal{E})}. \tag{2.12}$$

Algorithms satisfying eq. (2.12) with equality are said to be asymptotically optimal.

The Lai-Robbins bound is instance-dependent through its dependence on the Kullback-Leibler divergences. Its dependence on the divergences which are not known makes it inapplicable to real-world problems, and as reward distributions approach the optimal distribution, the bound diverges.

2.3.2 Instance-independent lower bound

A more general lower bound is the minimax regret. Given some problem class $\mathcal{E}$, it is defined as

$$\inf_{\pi} \sup_{\nu \in \mathcal{E}} R(\nu, \pi), \tag{2.13}$$

where π is the algorithm and ν is the problem instance. The minimax regret is a lower bound on the whole class rather than one particular instance; algorithms may achieve better in some or even most instances, but no algorithm can do better than the minimax regret in all. In [10], it is proven that for all algorithms, given a fixed horizon T and number of arms K, there is at least one problem instance such that

$$R_T = \Omega(\sqrt{KT}), \tag{2.14}$$

Such a bound is independent of the reward distributions, and as such, it is applicable in practice, but it may be overly robust. It can be preferable to sacrifice performance on some instances to gain performance on others. Minimax regret optimality implies a flat risk profile, while in practice, performance may be desired to correlate with instance difficulty. Surprisingly, minimax optimality does not negate instance optimality, and recent algorithms have been shown to achieve both [11, 12].

2.3.3 Bayesian optimality

If a prior distribution were to be placed on the reward distributions, a notion of average or Bayesian regret can be defined. For some bandit class $\mathcal{E}$, one simply includes the distribution of the reward distributions in the expectation taken to define the regret,

$$\mathrm{BR}_T(Q, \pi) = \mathbb{E}_{\pi,\nu,Q} \left[\sum_{a \in \mathcal{A}} \Delta_a T_a \right] = \mathbb{E}_{\nu \sim Q} \left[R_T(\nu, \pi) \right], \tag{2.15}$$

where Q is the prior distribution over $\mathcal{E}$. Is it trivially observed that the Bayesian regret bounded above by the minimax regret. However, it can be proven that there exists priors such that the Bayesian regret is bounded below by some $\Omega(\sqrt{KT})$, such that $\sup_Q \inf_\pi \mathrm{BR}_T(Q, \pi) = \Theta(\sqrt{KT})$ [7]

The Bayesian regret can be a useful tool for designing algorithms, as knowledge inlaid in the prior can be used to guide the algorithm, but it may lead to less robust designs than policies devised by the above discussed methods. Furthermore, calculating the optimal policy is generally intractable for any horizon of size and reward distributions more complicated than Bernoulli [7]. In simpler cases, dynamic programming can be fruitful. For longer horizons, discounting, namely reducing the weight of future rewards, can be used to make the problem tractable.

Table 2.3: Comparison of strategies.

Strategy	Regret	Tuning
Random	Linear	NA
Greedy	Linear	NA
Epsilon-greedy	Linear	Difficult
Epsilon-decay	Logarithmic	Difficult
UCB	Logarithmic	Barely
Thompson	Logarithmic	Priors

2.4 Strategies

2.4.1 Explore-only

Pure exploration is obviously a suboptimal strategy, but it is a good baseline against which to compare. It can be implemented by selecting an arm uniformly or in order, performing poorly either way. A random arm-selection procedure is described by algorithm 1.

Algorithm 1 Random arm selection

    Sample a from $\mathcal{A}$ uniformly
    return a

It is easy that the regret is

$$R_T = T\left(\mu^* - \frac{1}{k}\sum_{i=1}^{k}\mu_i\right), \tag{2.16}$$

which is necessarily linear in T. This motivates the search for an algorithm with sublinear regret.

2.4.2 Greedy

Tending away from pure exploration to exploitation, a greedy algorithm will always select the arm with the highest empirical mean. Here, all arms are pulled an initial $m \geq 1$ times, after which estimated means are used to select the best arm. Then, the arm with the highest empirical mean is selected for all remaining turns. The arm-selection procedure is listed in algorithm 2, where $\hat{\mu}_a$ is the estimated mean of arm a.

Algorithm 2 Greedy arm selection

---
  if $t \le mk$ **then**
    | **return** $(t \mod k) + 1$
  else
    | **return** $\text{argmax}_{a \in \mathcal{A}} \hat{\mu}_a$

With greedy selection, the expected regret is clearly still linear in the horizon, as there is a non-zero probability of selecting the wrong arm. Still, there is a chance of achieving zero regret and the constant factor is reduced compared to pure exploration selection. To improve hereupon, it is necessary to occasionally explore other arms, which leads into the epsilon-greedy algorithm.

2.4.3 Epsilon-greedy

The problem with the greedy algorithm is that it may be unlucky and not discover the best arm in the initial exploration phase. To mitigate this, the epsilon-greedy algorithm can be used. In this algorithm, the arm that is presumed to be best is pulled with probability $1 - \epsilon$, while in the other ϵ proportion of the turns, the arm is selected uniformly at random. This ensures convergence to correct exploitation as the horizon increases, and it will generally reduce the regret.

Still, with a constant ϵ, a constant proportion of the turns will be spent exploring, keeping the regret necessarily linear in the horizon. Choosing ϵ is a trade-off between exploration and exploitation and can significantly affect the regret.

Algorithm 3 Epsilon-greedy arm selection

---
  if $t \le mk$ **then**
    | **return** $(t \mod k) + 1$
  else
    Sample u from $[0, 1)$ uniformly
    if $u < \epsilon$ **then**
      | Sample a from $\mathcal{A}$ uniformly
      | **return** a
    else
      | **return** $\text{argmax}_{a \in \mathcal{A}} \hat{\mu}_a$

Epsilon-decay

To remedy the linear term in the regret, modifications to the epsilon-greedy algorithm have been proposed wherein ϵ is a function of the current time step t. Specifically, in order to achieve sublinear regret, it is necessary to decay ϵ towards zero. Decreasing ϵ over time makes intuitive sense; exploration is more crucial in the beginning stages of the algorithm, whereas exploitation is more important when the agent has more reliable estimates of the reward means. For example, one successful strategy is to set $\epsilon \sim 1/t$, which has been shown to achieve logarithmic instance-dependent regret [13]. It is worth noting, however, that the optimal decay rate depends on the specific instance, and achieving logarithmic regret can be challenging in practice [14].

2.4.4 Upper confidence bounds

The upper confidence bound (UCB) algorithm is a more sophisticated algorithm based on estimating an upper bound for the mean of each arm. One always chooses the arm whose upper confidence bound is highest, a principle known as 'optimism in the face of uncertainty'. This should make sense, as if the wrong arm appears best, it will be pulled more often and the empirical mean will be corrected, while the true best arm with its larger bound will eventually become highest and so pulled. When exploiting the actual best arm, the agent can trust it to be the best, as the confidence bound will remain above those of all the other arms. In addition, by increasing the confidence bounds as the number of pulls increases, getting stuck in suboptimality is avoided.

Assuming rewards in $[0, 1]$ and using Hoeffding's inequality, one has

$$p = P(\mu_a > \hat{\mu}_a + \mathrm{UCB}_a) \leq \exp\big(-2T_a \mathrm{UCB}_a^2\big), \qquad (2.17)$$

where UCB_a is the upper confidence bound for arm a and T_a is the number of times arm a has been pulled. Solving for UCB_a gives

$$\mathrm{UCB}_a = \sqrt{\frac{-\ln p}{2T_a}}. \qquad (2.18)$$

Letting $p(t) = t^{-4}$ gives

$$\mathrm{UCB}_a = \sqrt{\frac{2\ln t}{T_a}}, \qquad (2.19)$$

which is a common choice for the upper confidence bound, leading to the

14

UCB1-algorithm. In [13], it is shown that UCB1 achieves

$$R_T \leq \left(8 \sum_{a \in \mathcal{A} \backslash a^*} \frac{\log T}{\Delta_a} \right) + \left(1 + \frac{\pi^2}{3} \right) \sum_{a \in \mathcal{A}} \Delta_a, \qquad (2.20)$$

which only misses instance-dependent optimality by some constant factor. Nor is UCB1 truly minimax-optimal, is its instance-independent upper bound is $O(kT \log T)$ [14].

Regardless of the assumptions made and the bandit class, the procedure follows as in algorithm 4.

Many variants of the algorithm exist; different assumptions about the distributions change the confidence bounds. While the choice of p is arbitrary, it is less of nuisance than the choice of ϵ in the epsilon-greedy algorithm, with specific choices of p, such as the UCB1-algorithm, being well-studied and known to perform well. For example, MOSS, a modification of UCB1, has be shown to minimax-optimal for $\mathcal{E}_{[0,1]}^k$ [15]. Further, incorporating estimates of second moments improve performance in some cases [16], while incorporating the whole empirical distributions of observed rewards appears be the most effective approach [17].

Algorithm 4 UCB arm selection

---

   if $t \leq k$ **then**
      return t
   else
      return $\mathrm{argmax}_{a \in \mathcal{A}}(\hat{\mu}_a + \mathrm{UCB}_a)$

2.4.5 Thompson sampling

Thompson sampling is a Bayesian approach to the multi-armed bandit problem, being the original approach to the problem [2] in 1933, though only in the case of two arms and Bernoulli rewards and without any theoretical guarantees. This method is noteworthy for its ability to incorporate Bayesian modelling concepts into the fundamentally frequentist problem of multi-armed banditry. The idea is to sample from the posterior distribution of the means of the arms and pull the arm with the highest sample.

It was first in 2012 that Thompson sampling was proven asymptotically optimal for Bernoulli rewards with uniform priors [18]. Namely, for every $\epsilon > 0$, there exists a constant C_ϵ such that

$$R_T \leq (1 + \epsilon) \sum_{a \in \mathcal{A} \backslash a^*} \Delta_a \frac{\log T - \log \log T}{D(P_a \parallel P^*)} + C_\epsilon, \qquad (2.21)$$

where P_a is the reward distribution of arm a and P^* is the reward distribution of the best arm. Meanwhile, the minimax regret is can be bounded by either $O(\sqrt{kT\log T})$ [19] or $O(\sqrt{kT\log k})$ [20], neither of which is quite minimax-optimal.

Also for Gaussian rewards, it was proven asymptotically optimal with uniform priors [21]. Notably, the Jeffreys prior was shown to be inadequate in achieving optimal regret, highlighting the importance of the prior selection for the algorithm's performance.

Algorithm 5 Thompson sampling arm selection

---

for $a \in \mathcal{A}$ **do**
$\quad\lfloor$ Sample $\theta_a \sim P(\mu_a \mid \mathcal{D})$
return $\operatorname{argmax}_{a \in \mathcal{A}} \theta_a$
Update posterior for arm a with reward X_t

One of the key advantages of Thompson sampling is that it can natively incorporate prior knowledge about the arms, whereas doing so with the above methods would require some sort of ad-hoc manipulation of the recorded rewards and arm pulls. Furthermore, empirical results generally indicate better performance than UCB variants [18]. Still, Thompson sampling is not without its drawbacks. The algorithm can be computationally expensive, as it requires sampling from the posterior distribution for each arm at each time step. Even with conjugate priors, the computational costs of sampling will be higher than the simple computations required by UCB and epsilon-greedy algorithms.

2.4.6   The doubling trick

Given an algorithm reliant on knowing the horizon T, it is possible to use the doubling trick to achieve similar regret regardless of the horizon, creating an anytime algorithm. The doubling trick is a simple idea: simply first run the algorithm for T steps, then $2T$ steps, $4T$ ad infinitum, possibly with some other geometric factor. It was first introduced in [22], and has since been proven to conserve minimax regrets, but not instance-dependent regrets [23]. Using instead exponential progression, it is possible to maintain instance-dependent regret bounds instead of minimax optimality [23].

Chapter 3

Quantum computing

The field of quantum computing is split into two main branches: the development of quantum hardware and the study of algorithms that use such hardware. Only the second branch is relevant for this thesis, and even so only a brief explanation is offered here. For more details, see [24] for a rigorous, complete description or [25] for an introduction focused on programming. Any reader should have a basic understanding of linear algebra and classical computing. Knowledge of quantum mechanics is not assumed, albeit certainly helpful.

3.1   Quantum states

3.1.1   The qubit

The quantum bit, the qubit, is the building block of quantum computing. Like the classical binary digit, it can be either 0 or 1. But being quantum, these are quantum states, $|0\rangle$ and $|1\rangle$[1], and the qubit can be in any superposition of these states. This follows from the first postulate of quantum mechanics[2], which states that an isolated system is entirely described by a normalised vector in a Hilbert space. For the qubit, this is the two-dimensional space where the states $|0\rangle$ and $|1\rangle$ are basis vectors, known as the computational basis states. Thus, the state of a qubit can be

---

[1] The $|\cdot\rangle$ notation is known as a ket and is used in quantum mechanics to denote a quantum state. It is effectively a column vector. The inner product may be taken with a bra, $\langle\cdot|$, to give a scalar. These inner products are then denoted by $\langle\cdot|\cdot\rangle$. Similarly, outer products are well-defined and denoted by $|\cdot\rangle\langle\cdot|$.

[2] As they are laid out in [24].

expressed as

$$|\psi\rangle = \alpha\,|0\rangle + \beta\,|1\rangle = \begin{pmatrix} \alpha \\ \beta \end{pmatrix}, \tag{3.1}$$

where $\alpha, \beta \in \mathbb{C}$. The only requirement is that the state is normalised, $|\alpha|^2 + |\beta|^2 = 1$. Normalisation is required due to the Born rule, as the absolute square of the coefficients is the probability of measuring the qubit in the corresponding basis state.

3.1.2 The Bloch sphere

A useful tool for visualising the state of a qubit is the Bloch sphere. First, it should be noted that states on the form eq. (3.1) are not physically unique, only the relative complex phase matters. There is a global phase which can not be observed, and so it is not physically relevant. Taking that and the normalisation into account, the state of the qubit can be expressed as

$$|\psi\rangle = \cos\left(\frac{\theta}{2}\right)|0\rangle + e^{i\phi}\sin\left(\frac{\theta}{2}\right)|1\rangle, \tag{3.2}$$

where $\theta, \phi \in \mathbb{R}$. Interpreting θ as the polar angle and ϕ the azimuthal angle, the state of the qubit can be identified with a point on a sphere. See fig. 3.1. The state $|0\rangle$ is typically thought of as the north pole of this sphere and $|1\rangle$ the south pole.

3.1.3 Mixed states and density operators

It is not only the superpositions of states that are important in quantum computing, but also the mixed states, states that are statistical ensembles of pure states. Pure states are those expressible as a single ket like eq. (3.1), while mixed states arise when the preparation the system is not perfectly known or when the system interacts with the environment. For the description of mixed states, the formalism of density operators is more useful than the state vector formalism. If there are no classical uncertainties, the state is pure, and the density operator can be expressed a single ket-bra, $\rho = |\psi\rangle\langle\psi|$. In a mixed state, however, some classical probabilities p_i are associated with the different pure states $|\psi_i\rangle$, and the state of the system is described by the density operator

$$\rho = \sum_{i=1}^{n} p_i\,|\psi_i\rangle\langle\psi_i| \tag{3.3}$$
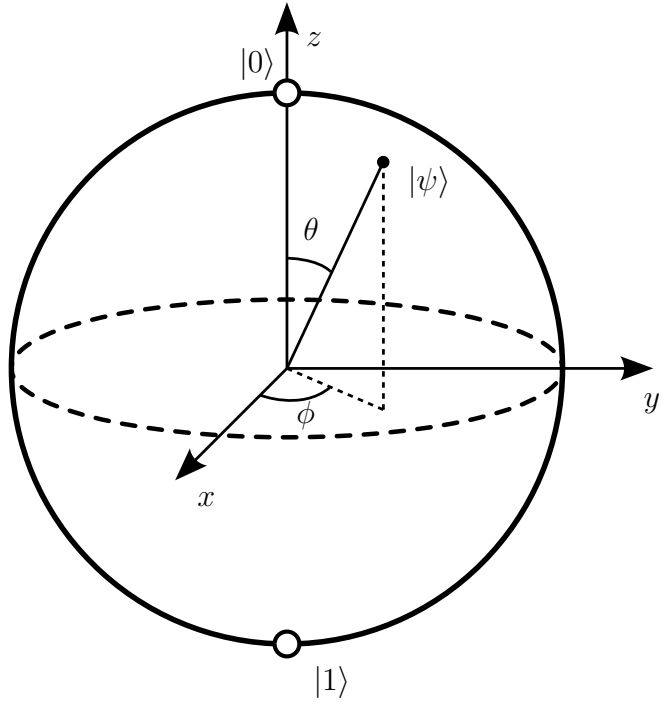
18

Figure 3.1: The Bloch sphere. On it, the state of a single qubit state is represented by a point. The state $|0\rangle$ is the north pole, and $|1\rangle$ is the south pole. The latitudinal angle θ determines the probability of measuring the qubit in the state $|0\rangle$, while the longitudinal angle ϕ corresponds to the complex phase between the two basis states. From [26].

where $|\psi_i\rangle$ are the states of the system, and $\langle\psi_i|$ are the corresponding dual vectors. Being probabilities, the p_i must be non-negative and sum to one. Given a basis and a finite Hilbert space, the density operator can be expressed as a density matrix[3] where the diagonal elements are the probabilities of measuring the system in the corresponding basis state. Furthermore, it is easily seen that the density operator must be positive semidefinite and Hermitian.

The Pauli matrices,

$$\sigma_x = \begin{pmatrix} 0 & 1 \\ 1 & 0 \end{pmatrix}, \quad \sigma_y = \begin{pmatrix} 0 & -i \\ i & 0 \end{pmatrix}, \quad \sigma_z = \begin{pmatrix} 1 & 0 \\ 0 & -1 \end{pmatrix}, \tag{3.4}$$

together with the identity matrix serve as a basis for the real vector-space of Hermitian 2×2-matrices. Since the diagonal elements of a density matrix must sum to one, the density matrix for a single qubit can be expressed as

$$\rho = \frac{1}{2} \left(I + x\sigma_x + y\sigma_y + z\sigma_z \right), \tag{3.5}$$

where $x, y, z \in \mathbb{R}$. Being positive semidefinite, the determinant should be non-negative, and thus it can be shown that $x^2 + y^2 + z^2 \leq 1$. This allows density operators to be interpreted as points on the Bloch sphere or indeed within it. Notably, pure states lie on the surface, while mixed states lie within the sphere (or rather, the Bloch ball). A pure quantum superposition of $|0\rangle$ and $|1\rangle$ with equal probabilities would have a complex phase and lie somewhere on the equator, while a statistical mixture with equal classical probabilities of being $|0\rangle$ and $|1\rangle$ would lie in its centre.

3.1.4   Systems of multiple qubits

Although the continuous nature of the qubit is indeed useful, the true power of quantum computers lie in how multiple qubits interact. Having multiple qubits enables entanglement, which is a key feature of quantum computing.

With two qubits, there are four possible states, $|00\rangle, |01\rangle, |10\rangle, |11\rangle$. Each of these four states have their own probability amplitude, and thus their own probability of being measured. A two-qubit system will therefore operate with four complex numbers in the four-dimensional Hilbert space $\mathbb{C}^4$.

---

[3]Density operators and matrices are often used interchangeably in quantum computing. Due to the finite number of qubits, the Hilbert spaces are always finite-dimensional, and with the canonical basis, there is a canonical way of representing density operators as matrices.

Generally, the state of multiple qubits can be expressed using the tensor product as

$$|\psi_1\psi_2\cdots\psi_n\rangle = |\psi_1\rangle\,|\psi_2\rangle\cdots|\psi_n\rangle = |\psi_1\rangle\otimes|\psi_2\rangle\otimes\cdots\otimes|\psi_n\rangle. \qquad (3.6)$$

What makes this so powerful is that the state of a multi-qubit system has the general form

$$\begin{aligned}
|\psi_1\psi_2\cdots\psi_n\rangle &= c_1\,|0\ldots00\rangle + c_2\,|0\ldots01\rangle + \cdots + c_{2^n}\,|1\ldots11\rangle \\
&= (c_1, c_2, \ldots, c_{2^n})^\top \\
&\in \mathbb{C}^{2^n},
\end{aligned} \qquad (3.7)$$

which means that with n qubits, the system can be in any superposition of the 2^n basis states. Operating on several qubits then, one can do linear algebra in an exponentially large space. This is a key part of the exponential speed-ups possible with quantum computers.

3.2 Quantum operations

3.2.1 Single-qubit gates

To operate on one or more qubits, a unitary operation is applied to the state. This is a computational interpretation of the unitary time evolution resulting from a Hamiltonian acting on the (closed) quantum system, described by the second postulate of quantum mechanics and the Schrödinger equation. As the operations are unitary, a pure state remains pure. These operations are often thought of as gates, paralleling the classical gates in digital logic. Mathematically, with a finite number of qubits, a unitary gate U can be expressed as matrices acting on the state vector, $|\psi\rangle$, as

$$|\psi'\rangle = U\,|\psi\rangle, \qquad (3.8)$$

where $|\psi'\rangle$ is the resulting state.

The most basic gates are the Pauli gates, which are applications of the Pauli matrices from eq. (3.4) and are as gates simply denoted as X, Y, and Z. These gates can be seen as half turns around the x-, y- and z-axes, respectively, of the Bloch sphere. The X-gate is also known as the NOT gate, as it mirrors the classical NOT gate by mapping $|0\rangle$ to $|1\rangle$ and vice versa. It is however more general, being also applicable to superposition states.

The Hadamard gate,

$$H = \frac{1}{\sqrt{2}} \begin{pmatrix} 1 & 1 \\ 1 & -1 \end{pmatrix},$$ (3.9)

is a rotation around the line between the x- and z-axes by $\pi/2$. It is an important gate in quantum computing, as it is used to create superpositions of the computational basis states. Applied on an initial $|0\rangle$ state, it creates the entangled state $\frac{1}{\sqrt{2}}(|0\rangle + |1\rangle)$. Two consecutive applications thereof returns the state to the initial state, as can be seen from the matrix squaring to the identity.

The R_X-, R_Y- and R_Z-gates are rotations around the x-, y- and z-axes, respectively, by an arbitrary angle θ:

$$R_X(\theta) = \begin{pmatrix} \cos\left(\frac{\theta}{2}\right) & -i\sin\left(\frac{\theta}{2}\right) \\ -i\sin\left(\frac{\theta}{2}\right) & \cos\left(\frac{\theta}{2}\right) \end{pmatrix},$$

$$R_Y(\theta) = \begin{pmatrix} \cos\left(\frac{\theta}{2}\right) & -\sin\left(\frac{\theta}{2}\right) \\ \sin\left(\frac{\theta}{2}\right) & \cos\left(\frac{\theta}{2}\right) \end{pmatrix},$$

$$R_Z(\theta) = \begin{pmatrix} e^{-i\frac{\theta}{2}} & 0 \\ 0 & e^{i\frac{\theta}{2}} \end{pmatrix}.$$

These parametrised gates will be useful in **??**.

3.2.2 Multi-qubit gates

Multi-qubit gates are gates that act non-trivially on more than one qubit. The most used multi-qubit gate is the controlled X-gate, also known as the CNOT. Being controlled means that it only acts on the second qubit if the first qubit is in the state $|1\rangle$. Of course, the first qubit may be in a superposition, and the CNOT this way allows for the creation of entanglement between the two qubits. If the first qubit has probability amplitude α of being in the state $|1\rangle$, the second qubit will have probability amplitude α of being flipped. The CNOT-gate, acting on the leftmost qubit in the tensored two-qubit system can be expressed in matrix form as

$$\text{CNOT} = \begin{pmatrix} 1 & 0 & 0 & 0 \\ 0 & 1 & 0 & 0 \\ 0 & 0 & 0 & 1 \\ 0 & 0 & 1 & 0 \end{pmatrix}.$$ (3.10)

In theory, any unitary single-qubit operation can be controlled. However, it is often only the CNOT that is used is implemented in the hardware.

Another interesting two-qubit gate is the controlled Z-gate, CZ, expressible as the matrix

$$\text{CZ} = \begin{pmatrix} 1 & 0 & 0 & 0 \\ 0 & 1 & 0 & 0 \\ 0 & 0 & 1 & 0 \\ 0 & 0 & 0 & -1 \end{pmatrix}. \tag{3.11}$$

Because it only alters the amplitude of $|11\rangle$, it does not actually matter which qubit is the control and which is the target.

3.2.3 Observables and measurements

For an output to be obtained from a quantum computer, a measurement must be performed. This is typically done at the end of all operations and of all qubits, where each qubit is measured in the computational basis to yield a string of bits.

As described by the third postulate of quantum mechanics, any observable quantity has a corresponding Hermitian operator A, spectrally decomposable as $A = \sum_i \lambda_i P_i$, where λ_i are the (necessarily real) eigenvalues and P_i are the corresponding projectors onto the eigenspaces. When measuring, the probability of obtaining the outcome λ_i is given by

$$p_i = \langle \psi | P_i | \psi \rangle, \tag{3.12}$$

where $|\psi\rangle$ is the state before the measurement. It is one of Nature's great mysteries what exactly a measurement is and even more so how and why it is different from the unitary evolution described by the second postulate. In the quantum computational setting, it can be thought of as taking a random sample with the probabilities as given by the above equation.

Often, the underlying probabilities are what is of interest. Therefore, many measurements will be performed. Usually, these results are averaged to obtain an estimate, but more complicated post-processing methods are also possible. For instance, neural networks have shown useful properties in regard of reducing variance in the estimates, though at the cost of some bias [27].

Canonically, the computational Z-basis is used for measurements, and it is usually the only basis for which measurements are physically implemented in a quantum computer. When measuring in the computational basis in which a state is expressed, as eq. (3.7), the probabilities are simply given by the absolute square of the coefficients. To virtually measure another observable, a change of basis is performed. This is achieved by applying a unitary transformation before measurement.

Measurements may be done in the middle of a computation and be used to control gates. If the qubits are entangled, measuring one will affect the measurement probabilities of others. Using such intermediate measurements is a way of introducing non-linearities in the otherwise unitary nature of the unmeasured quantum world.

3.2.4 Quantum circuits

The operations on qubits are often described using quantum circuits, which are a graphical representation of the operations on the qubits, the quantum algorithms. They are read from left to right. It is standard procedure to assume all qubits start in the state $|0\rangle$. Gates are generally written as boxes with the name of the gate inside.

A simple example is the circuit

$$|0\rangle \; -\boxed{H}- \\ |0\rangle \; -\boxed{H}- \tag{3.13}$$

which prepares the state $\frac{1}{2}(|00\rangle + |01\rangle + |10\rangle + |11\rangle) = \frac{1}{\sqrt{2}}(|0\rangle + |1\rangle) \otimes \frac{1}{\sqrt{2}}(|0\rangle + |1\rangle)$. This is a pure state with no entanglement, and so the measurement probabilities of the two qubits are independent. When measured, all four outcomes are equally likely.

Slightly more interesting is the circuit

$$|0\rangle \; -\boxed{H}-\bullet- \\ |0\rangle \; -\!\!\oplus\!\!- \tag{3.14}$$

in which the first qubit is put into a superposition using the Hadamard gate before a CNOT gate is applied to the second, controlled by the first. This creates the state $\frac{1}{\sqrt{2}}(|00\rangle + |11\rangle)$. The measurement probabilities of the two qubits are now correlated; if the first qubit is measured to be $|1\rangle$, the second will always be $|1\rangle$ and vice versa. The probability of measuring the qubits to be different is nil.

To create a mixed state, an intermediate measurement can be used to control a gate. For instance, the circuit

$$|0\rangle \; -\boxed{H}-\boxed{\nearrow}-\bullet- \\ |0\rangle \; -\boxed{X}- \tag{3.15}$$

places the second qubit in the mixed state $\frac{1}{2}(|0\rangle\langle 0| + |1\rangle\langle 1|)$. If it were immediately to be measured, it would have a 50% chance of being $|0\rangle$ and a 50% chance of being $|1\rangle$. The uncertainty is only classical, and it could therefore not be used to create entanglement or for any other quantum spookiness.

3.2.5 Quantum supremacy

Exponential speed-ups do not come for free. Although the states spaces are exponentially large, with only a limited set of operations available, states can not be created and manipulated arbitrarily; the problem must have some structure to be exploited for a speed-up to be possible. Quantum computers do only solve certain problems more efficiently than classical computers, and finding the algorithms to do so is not trivial. Shor's algorithm has time complexity $O((\log N)^3)$ while the most efficient known classical algorithm, the general number field sieve, is sub-exponential with a time complexity on the form $\Omega(k^{\frac{1}{3}} \log^{2/3} k)$, where $k = O(2^N)$ [28]. To solve linear system, there is the HHL algorithm with time complexity $O(\log(N)\kappa^2)$, where κ is the condition number. This is an exponential speed-up over the fastest known classical algorithm[4], which has time complexity $O(N\kappa)$. Still, these are non-trivial algorithms, not yet usable in practice and that were not easily found.

Polynomial speed-ups are perhaps more easily found. For example, the Grover algorithm which is used to search for an element in an unsorted list has time complexity $O(\sqrt{N})$ [30]. Classically, this can not be done in less than $O(N)$ time. It can be proven that the Grover algorithm is optimal [31], so for this problem, an exponential speed-up is impossible. This algorithm and the more general amplitude amplification on which it builds solves very general problems and are often used subroutines to achieve quadratic speed-ups in other algorithms. Being only a quadratic speed-up, it is not as impressive as the exponential speed-ups, and achieving quantum supremacy in that manner would require larger quantum computers than if the speed-up were exponential.

It is proven that the class of problems quantum computers can solve in polynomial time (with high probability), BQP, contains the complexity class P [24]. This follows from the fact than quantum computers run do any classical algorithm. Since quantum computers can solve problems like

---

[4]Given that the condition number does not grow exponentially. There are also difficulties in loading the data into the quantum computer and extracting the solution that could negate any exponential speed-up. C.f. [29].

integer factorisation and discrete logarithms efficiently, it is believed that BQP is strictly greater than P, but as whether P = NP remains unknown, these problems could actually be in P. In a similar vein, NP-complete problems are believed to lie outside BQP.

3.3 Quantum algorithms

3.3.1 Grover's algorithm

The quantum search algorithm of Grover [30] is a quantum algorithm that finds an element in an unstructured list with high probability. While such a problem necessarily requires $O(N)$ time in a classical setting, needing on average $N/2$ steps to find the element and in the worst case N, Grover's algorithm finds the element in $O(\sqrt{N})$ steps. This is a quadratic speed-up.

Grover's algorithm is provably optimal; no quantum algorithm can perform such general searches faster [31]. This should not be surprising. If an exponential speed-up were possible, Grover search could be used to find the solution to NP-hard problems fast.

For Grover's algorithm to work, assume there is a function f that maps the index of an element to 1 if it is the one desired and 0 otherwise. Then, one assumes access to a quantum oracle, $\mathcal{O}_f$ (effectively a black box subroutine) that implements f thus:

$$\mathcal{O}_f \left| x \right\rangle = (-1)^{f(x)} \left| x \right\rangle. \tag{3.16}$$

A single application of this oracle is not enough to find the desired element, as the square of the amplitude of the desired element remains unchanged. Central to Grover's algorithm is the idea of amplifying the amplitude of the desired element. This is done by applying a sequence of operations that is repeated until the amplitude of the desired element is large enough for it is most likely to be measured, while the amplitudes of the other elements are reduced.

Let the state $\left| w \right\rangle$ which be the winner state, a state with amplitude 1 for the desired element and 0 for all others. Then consider the state $\left| s \right\rangle$, which is a uniform superposition state, a state with equal amplitudes for all elements. Define the state $\left| s' \right\rangle$ by subtracting the projection of $\left| w \right\rangle$ onto $\left| s \right\rangle$ from $\left| s \right\rangle$:

$$\left| s' \right\rangle = \left| s \right\rangle - \left\langle w | s \right\rangle \left| w \right\rangle. \tag{3.17}$$

These two orthogonal states form a basis of a two-dimensional subspace of the greater Hilbert space. This permits a perspicuous visualisation of the

algorithm, as in fig. 3.2. The uniform superposition state $|s\rangle$ serves as a starting point for the algorithm, and is achieved by applying Hadamard gates to all qubits. It is expressible as

$$|s\rangle = \cos(\theta) |s'\rangle + \sin(\theta) |w\rangle, \tag{3.18}$$

where $\theta = \arcsin \langle s|w\rangle = \arcsin(1/\sqrt{N})$.

Applying the oracle on $|s\rangle$ leaves its $|s'\rangle$ component unchanged, but flips the sign of the $|w\rangle$ component. This results in the state $|\psi\rangle = \cos(-\theta) |s'\rangle + \sin(-\theta) |s'\rangle$, which can be seen as reflection of $|s\rangle$ in the $|s'\rangle$ direction.

Next, the state $|\psi\rangle$ is reflected about the initial $|s\rangle$ state, resulting in the state $|\psi'\rangle = \cos(3\theta) |s'\rangle + \sin(3\theta) |w\rangle$. Reflection thus is achieved by the diffusion operator

$$D = H^{\otimes n} S_0 (H^{\otimes n})^{-1} = H^{\otimes n} S_0 H^{\otimes n}, \tag{3.19}$$

where $S_0 = 2 |0\rangle\langle 0| - I$ is the reflection operator about the $|0\rangle$ state, that is an operator that flips the sign of all but the $|0\rangle$ component.

The product of the oracle and the diffusion operator defines the Grover operator, which is simply applied until the amplitude of the $|w\rangle$ is sufficiently amplified. After k iterations, the state is $|\psi_k\rangle = \cos((2k+1)\theta) |s'\rangle + \sin((2k+1)\theta) |w\rangle$. Measuring the correct state has probability $\sin^2((2k+1)\theta)$. Therefore, $k \approx \pi/4\theta$ iterations should be completed. Assuming large N, for a short list would not warrant the use of Grover's algorithm, $\theta = \arcsin(1/\sqrt{N}) \approx 1/\sqrt{N}$, and so $k \approx \pi\sqrt{N}/4$.

For lists with more than a single desired element, a similar reasoning will lead to the same algorithm, but instead with $k \approx \pi/4\sqrt{N/M}$, where M is the number solutions to $f(x) = 1$ [24].

3.3.2   Amplitude amplification

Amplitude amplification can be considered a generalisation of Grover's algorithm. Instead of a single oracle, let the partitioning of the state space be given by a Hermitian projector P, whose image will be the space of states to amplify. Then, for some given initial state $|\psi\rangle$, it is decomposed into the orthogonal components

$$|\psi\rangle = \sin(\theta) |\psi_0\rangle + \cos(\theta) |\psi_1\rangle, \tag{3.20}$$

where $|\psi_1\rangle = P |\psi\rangle$ and $|\psi_0\rangle = |\psi\rangle - |\psi_1\rangle$, effectively the projections onto the image and kernel of P. Clearly, the angle θ is given by $\arcsin(|P|\psi\rangle|)$.
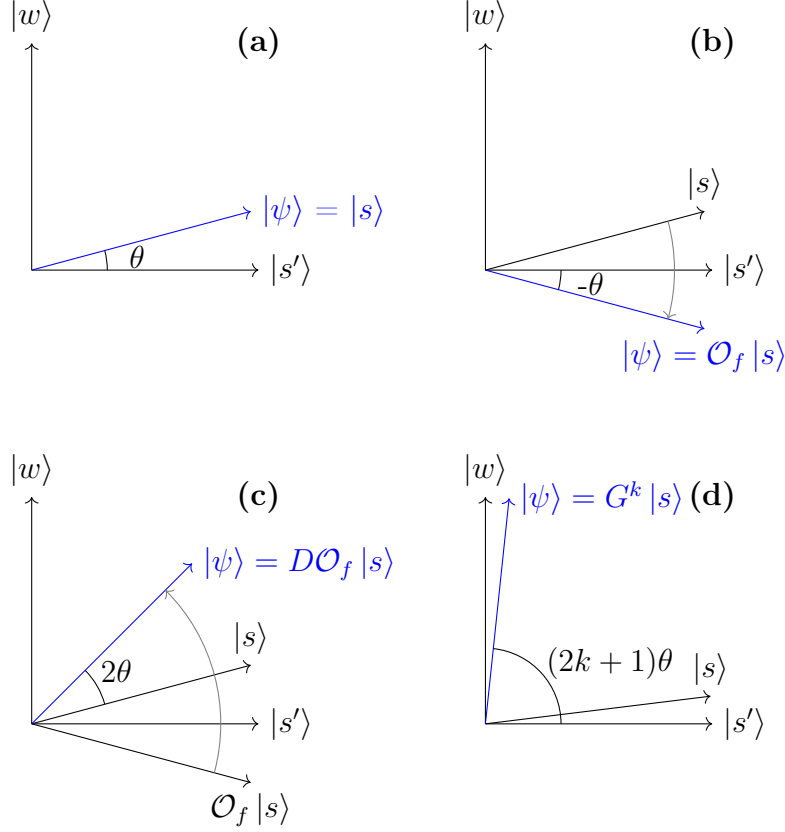
Figure 3.2: Grover's algorithm visualised. (a) The initial uniform superposition state $|s\rangle$ is prepared, which can be seen as a linear combination of $|w\rangle$ and $|s'\rangle$, forming an angle θ to the s'-axis. (b) The oracle $\mathcal{O}_f$ is applied to $|s\rangle$, flipping the sign of its $|w\rangle$ component, inverting the angle θ. (c) The diffusion operator D is applied, reflecting the state about the initial state and towards the goal, resulting in a state with an angle 3θ to the w-axis. (d) After repeating the previous two steps a k times, the angle is $2k + 1\theta$, and if k is chosen wisely, this means that the system is in a state close to the desired state $|w\rangle$, such that measuring the system will likely result in $|w\rangle$.

The Grover operator is now given by $G = -S_\psi S_P$ where

$$S_\psi = I - 2\,|\psi\rangle\,\langle\psi| \tag{3.21}$$

$$S_P = I - 2P, \tag{3.22}$$

such that S_ψ being analogue to the diffusion operator D and S_P being the oracle operator.

Following the same reasoning as in the previous section, the state after k iterations is given by

$$G^k\,|\psi\rangle = \sin((2k+1)\theta)\,|\psi_1\rangle + \cos((2k+1)\theta)\,|\psi_0\rangle, \tag{3.23}$$

meaning that $k \approx \frac{\pi}{4\theta}$ will result in a state close to $|\psi_1\rangle$.

Amplitude amplification can be used to speed up Grover search by using an informed prior rather than a uniform prior. Furthermore, it is useful as a subroutine in other algorithms, such as finding the number of 'good' states for a Grover search [32], quantum Monte Carlo methods [33] and some bandit algorithms to be discussed in what follows.

3.3.3 Amplitude estimation

As with amplitude amplification, amplitude estimation considers states that are decomposed into a superposition of two states, and, as the name suggests, estimates the amplitude of one of the states. Given a state, or more generally the algorithm, $\mathcal{A}$ with which it is generated,

$$\mathcal{A}\,|0\rangle = \sqrt{a}\,|\psi_1\rangle + \sqrt{1-a}\,|\psi_0\rangle, \tag{3.24}$$

where $|\psi_1\rangle$ is a state of interest and $|\psi_0\rangle$ its orthogonal complement, the goal is to estimate its amplitude $a = |\langle\psi_1|\psi_1\rangle|^2$.

With its original formulation in [32], it was proven that the amplitude can be estimated with an additive error of

$$\epsilon \le 2\pi \frac{\sqrt{a(1-a)}}{t} + \frac{\pi^2}{t^2} \tag{3.25}$$

with probability at least $8/\pi^2(\approx 81.06\%)$ using t calls to the algorithm $\mathcal{A}$. The probability can be increased to $1-\delta$, requiring $O(\log(1/\delta))$ calls to $\mathcal{A}$ [33]. Later variants have been proposed to reduce the qubits needed and circuit depths [34, 35, 36], making it more feasible for NISQ devices, while still achieving similar asymptotic error bounds.

3.3.4 Quantum Monte Carlo

Monte Carlo methods have been a powerful tool to analyse the behaviour of quantum mechanical systems, where probabilistic methods are natural to describe probabilistic physics [37, 38, 39]. On the other hand, more in line with the scope of this report, recent advances in quantum computing have opened up a new avenue for the intersection of quantum mechanics and Monte Carlo methods.

In the problem of estimating the mean of a random variable, the additive error can be bounded by Chebyshev's inequality as

$$P(|\hat{\mu} - \mu| \geq \epsilon) \leq \frac{\sigma^2}{n\epsilon^2}, \tag{3.26}$$

where $\hat{\mu}$ is the sample mean, μ is the true mean, σ is the standard deviation and n is the number of samples. Consequently, there is a need of quadratically many samples to achieve a given error, which for example means that estimating the mean of a random variable with a standard deviation of 1 with four decimals' accuracy and a certainty of 99.9% would require 10^9 samples. Moreover, this is provably optimal asymptotically [40].

Generalising amplitude estimation, in [33], a near-quadratic speed-up of Monte Carlo methods was achieved by using amplitude estimation to estimate the mean of a random variable encoded by quantum algorithms. Given an algorithm $\mathcal{A}$ whose outputs are assigned real values such that $v(\mathcal{A})$ is a random variable with mean μ and variance σ^2, it is proved that approximating μ with an additive error of ϵ can be achieved with only $\tilde{O}(\sigma/\epsilon)$ calls to $\mathcal{A}$ and its inverse, which is a near-quadratic speed-up over the classical case[5].

The simpler version on which the general builds, $v(\mathcal{A})$ is assumed to lie in the interval $[0, 1]$. Thus, the value can be encoded in a single qubit by through a unitary

$$W |x\rangle |0\rangle = |x\rangle \left(\sqrt{1 - \phi(x)} |0\rangle + \sqrt{\phi(x)} |1\rangle \right), \tag{3.27}$$

where $\phi(x)$ is the output of the algorithm were x to be measured. Thence, the amplitude is simply estimated using amplitude estimation with an appropriate number of repeats and iterations, where the initial state is $|\psi\rangle = W(\mathcal{A} \otimes I) |0\rangle$. In particular, for these bounded random variables, $O(1/\epsilon)$ iterations suffices to achieve an additive error of ϵ, repeating the whole procedure $O(1/\log(\delta))$ times to achieve a certainty $1 - \delta$ [33].

---

[5]The $\tilde{O}$ notation ignores logarithmic factors.

Chapter 4

Quantum bandits

Several formulations of the multi-armed bandit problem have been made for a quantum computing setting. As the central issue in bandit problems lie in sample efficiency rather than computational difficulties, quant-um computers offer little advantage assuming classical bandits. However, by granting some sort of superposition queries, means can be estimated more efficiently, and so regrets may be reduced, or best arms found more quickly.

Querying in superposition may at first appear to remove any real-world relevance; administering medications to patients can certainly not be done in superposition. However, with the training for reinforcement learning primarily being done in simulation, it is conceivable that the theory of quantum bandits may be applied to the learning of agents that are trained on quantum hardware and subsequently deployed to the real world.

4.1 Oracles as bandit arms

A way to quantise the bandit problem is to assign to each arm a quantum oracle. For each arm $a \in \mathcal{A}$, a bandit oracle can be defined as

$$\mathcal{O}_a : |0\rangle \otimes |0\rangle \mapsto \sum_{\omega \in \Omega} \left(\sqrt{P_a(\omega)} \, |\omega\rangle \otimes |X_a(\omega)\rangle \right), \qquad (4.1)$$

where ω is some sample space on which X_a is a random variable with probability measure P_a. Applying the oracle to the state $|0\rangle$ produces a superposition of all possible outcomes of the random variable X_a, such that measuring the second register will produce a sample from X_a. In this way, this quantum version of the bandit problem can be reduced to the classical case, but by maintaining the superposition, quantum advantages can be gained.

As with classical arms, the agent decides for each step in the bandit problem which oracle to invoke, trying to minimise the cumulative regret, where the means here are defined as

$$
\begin{aligned}
\mu_a &= \sum_{\omega \in \Omega} P_a(\omega) X_a(\omega) \\
&= \langle 00| \, \mathcal{O}_a^\dagger (I \otimes Z) \mathcal{O}_a) \, |00\rangle
\end{aligned}
\tag{4.2}
$$

In [41], an algorithm for bounded-value arms achieving $O(n \log T)$ regret was proposed, n being the number of arms. For bounded variances, the regret is $O(n \, \text{poly}(\log T))$, which is still substantially better than $\Omega(\sqrt{nT})$ minimax regret for classical bandits.

The algorithm proposed is essentially a UCB-like algorithm, where QMC (as described in section 3.3.4) is used to estimate means more efficiently. Because QMC estimates are only produced after a set number of quantum queries, the algorithm must cleverly decide for how many steps to pull each arm in addition to which arm to pull, before running a QMC session.

As listed in algorithm 6, the algorithm first runs a preliminary phase where the means are estimated using QMC with a fixed number of samples, after which it iteratively pulls the arms with the highest confidence bounds, after which the confidence bound are halved and the number of QMC samples to be used for that arm is doubled. A confidence parameter δ is used to determine the number of QMC samples to use, satisfying $|\hat{\mu}_i - \mu_i| \leq \text{UCB}_i$ with probability $1 - \delta$. The constant $C_1 > 1$ is only described existentially to give an upper bound to the number of QMC queries needed, coming from the big-O notation used to describe QMC convergence. How it should be set for implementation of the algorithm is not described in the paper.

Algorithm 6 QUCB1 as proposed in [41]

Require: Set of arms $\mathcal{A}$, $\mathcal{O}_i$ as in eq. (4.1), T horizon, $0 < \delta \ll 1$
1: **for** $a \in \mathcal{A}$ **do**
2:      $\text{UCB}_a \leftarrow 1$
3:      $N_a \leftarrow (C_1/\text{UCB}_a) \log(1/\delta)$
4:      Estimate μ_a using QMC with N_a samples
5: **while** Total number of queries to the oracles is less than T **do**
6:      $a \leftarrow \text{argmax}_a(\hat{\mu}_a + \text{UCB}_a)$
7:      $\text{UCB}_a \leftarrow \text{UCB}_a/2$
8:      $N_a \leftarrow (C_1/\text{UCB}_a) \log(1/\delta)$
9:      Update estimate of μ_a using QMC with N_a samples

4.1.1 Proof of logarithmic regret

Recall that for variables in $Y \in [0,1]$ producible by quantum algorithms, QMC can estimate $\mathbb{E}[Y]$ with error $|\hat{\mu} - \mu| \leq \epsilon$ with probability $1 - \delta$ using $\frac{C_1}{\epsilon} \log \frac{1}{\delta}$ queries or less to the oracle or its adjoint, for some universal constant $C_1 > 1$. That means that for each a,

$$|\hat{\mu}_a - \mu_a| \leq \mathrm{UCB}_a \quad \text{with probability} \quad 1 - \delta, \tag{4.3}$$

for each QMC session in the algorithm.

Let S_a be the set of stages where arm a is pulled in the while-block of the algorithm, and let its cardinality be $K_a = |S_a|$. Then, each arm is pulled $(2^{K_a+1} - 1)C_1 \log \frac{1}{\delta}$ in the second phase. With the preliminary phase, the total number of queries is

$$C_1 \log \frac{1}{\delta} \sum_{a \in \mathcal{A}} 2^{K_a+1} = T. \tag{4.4}$$

Further, using Jensen's inequality,

$$\sum_{a \in \mathcal{A}} 2^{K_a+1} \geq k 2^{1/k \sum_{a \in \mathcal{A}} (K_a+1)}, \tag{4.5}$$

it follows that

$$\sum_{a \in \mathcal{A}} K_a \leq k \log_2 \left(\frac{T}{kC_1 \log \frac{1}{\delta}} \right) - k, \tag{4.6}$$

which considering the first k rounds, gives that the total number of QMC sessions is

$$N_{\mathrm{QMC}} \leq k \log_2 \left(\frac{T}{kC_1 \log \frac{1}{\delta}} \right). \tag{4.7}$$

The probability of all QMC queries satisfying the error bound of eq. (4.3) is

$$
\begin{aligned}
1 - \left(\bigcup_{i=1}^{N_{\mathrm{QMC}}} P(\text{Query } i \text{ fail}) \right) &\leq 1 - \sum_{i=1}^{N_{\mathrm{QMC}}} P(\text{Query } i \text{ fail}) \\
&= 1 - \sum_{i=1}^{N_{\mathrm{QMC}}} \delta \\
&= 1 - N_{\mathrm{QMC}} \, P(\text{Query } i \text{ fail}) \\
&\leq k \log_2 \left(\frac{T}{kC_1 \log \frac{1}{\delta}} \right) \delta.
\end{aligned} \tag{4.8}
$$

33

Denote this event by E. For the a that is chosen in the argmax in line 6 of the algorithm,

$$\hat{\mu}_a + \mathrm{UCB}_a \geq \hat{\mu}^* + \mathrm{UCB}^*, \tag{4.9}$$

and given E, it generally holds that

$$\hat{\mu} \leq \mu + \mathrm{UCB} \quad \text{and} \quad \mu \leq \hat{\mu} + \mathrm{UCB}. \tag{4.10}$$

Hence, the suboptimality gap of arm a is bounded by

$$
\begin{aligned}
\Delta_a &:= \mu^* - \mu_a \\
&\leq (\hat{\mu}^* + \mathrm{UCB}^*) - (\hat{\mu}_a - \mathrm{UCB}_a) \\
&\leq (\hat{\mu}_a + \mathrm{UCB}_a) - (\hat{\mu}_a - \mathrm{UCB}_a) \\
&= 2\mathrm{UCB}_a.
\end{aligned} \tag{4.11}
$$

Notably, this holds regardless of what stage of the algorithm the arm is pulled in, so the last, most precise estimate of μ_a is used, wherein $\mathrm{UCB}_a = 2^{1-K_a}$. Consequently, the regret contribution of arm a is bounded by

$$
\begin{aligned}
T_a \Delta_a &\leq 2 T_a \mathrm{UCB}_a. \\
&= 2(2^{K_a+1} C_1 \log \frac{1}{\delta}) 2^{1-K_a} \\
&= 2^3 C_1 \log \frac{1}{\delta}.
\end{aligned} \tag{4.12}
$$

Given E, it is hence clear that

$$\sum_{a \in \mathcal{A}} T_a \Delta_a \leq 8(k-1) C_1 \log \frac{1}{\delta}. \tag{4.13}$$

In the case where E does not occur, the regret contribution can be bounded by

$$\sum_{a \in \mathcal{A}} T_a \Delta_a \leq T \max_{a \in \mathcal{A}} \Delta_a \leq T. \tag{4.14}$$

34

The regret can hence be bounded by

$$
\begin{aligned}
R_T &= \mathbb{E}\left[\sum_{a\in\mathcal{A}} T_a \Delta_a\right] \\
&= \mathbb{E}\left[\mathbb{E}\left[\sum_{a\in\mathcal{A}} T_a \Delta_a \,\middle|\, E\right]\right] \\
&= P(E)\mathbb{E}\left[\sum_{a\in\mathcal{A}} T_a \Delta_a \,\middle|\, E\right] + P(\neg E)\mathbb{E}\left[\sum_{a\in\mathcal{A}} T_a \Delta_a \,\middle|\, \neg E\right] \quad (4.15) \\
&\leq (1 - P(\neg E))\left(8(k-1)C_1 \log\frac{1}{\delta}\right) + P(\neg E)T \\
&\leq 8(k-1)C_1 \log\frac{1}{\delta} + P(\neg E)T. \\
&\leq 8(k-1)C_1 \log\frac{1}{\delta} + k\delta \log_2\left(\frac{T}{kC_1 \log\frac{1}{\delta}}\right)T.
\end{aligned}
$$

Setting $\delta = 1/T$,

$$
\begin{aligned}
R_T &\leq 8(k-1)C_1 \log\frac{1}{\delta} + k\log_2\left(\frac{T}{kC_1 \log\frac{1}{\delta}}\right) \\
&\leq 8(k-1)C_1 \log T + k\log_2\left(\frac{T}{kC_1 \log T}\right) \quad (4.16) \\
&\leq 8(k-1)C_1 \log_2 T + k\log_2 T \\
&= (8(k-1)C_1 + k)\log_2 T \\
&= O(k\log T)
\end{aligned}
$$

as desired.

4.2 Best arm identification

In [42], an algorithm based on amplitude amplification is proposed and is shown to find the optimal arm with quadratically fewer queries than the best classical algorithm for classical bandits in the case of Bernoulli rewards. There is albeit a significant drawback: the probability of the correct arm being suggested can not be set arbitrarily high, but is instead given by the ratio of the best arm's mean to the sum of the means of all arms. This greatly limits the usefulness of the algorithm, but it may still serve as a useful baseline for comparison, with the more complicated algorithms discussed in the following sections seeable as extensions hereof.

They assume access to an oracle $\mathcal{O}_e$ that encodes the probabilities of the arms,

$$\mathcal{O}_e : |a\rangle \otimes |0\rangle \mapsto |a\rangle \otimes \sum_{\omega \in \Omega} \sqrt{P_a(\omega)} \, |Y(\omega)\rangle \qquad (4.17)$$

where a is the arm to be queried, ω some state in the sample space Ω, $P_a(\omega)$ the probability measure thereon, from which the random variable $Y(\omega)$ is drawn, some internal state. For a given arm a and the internal state $|y\rangle$, the reward is determined by some function $f(a, y) \to \{0, 1\}$, accessed through the phase oracle $\mathcal{O}_f$,

$$\mathcal{O}_f : |a\rangle \otimes |y\rangle \mapsto (-1)^{f(x,y)} |a\rangle \otimes |y\rangle . \qquad (4.18)$$

For such bandits, regret minimisation is no longer a valid objective, as all arms are in a sense pulled simultaneously. Instead, the problem is to find a strategy that maximises the probability of finding the optimal arm with as few applications of $\mathcal{O}_e$ as possible.

The authors of [43] propose a more sophisticated algorithm, improving the results of [42] by allowing the probability of finding the optimal arm to be set arbitrarily high. Theirs is also quadratic speed-up over the best classical algorithm, but is more complicated and requires a quantum computer with more qubits.

36

References

[1] Herbert Robbins. 'Some Aspects of the Sequential Design of Experiments'. In: *Bulletin of the American Mathematical Society* 58.5 (1952), pp. 527–535. DOI: `10.1090/S0002-9904-1952-09620-8`. URL: `https://www.ams.org/bull/1952-58-05/S0002-9904-1952-09620-8/`.

[2] William R. Thompson. 'On the Likelihood That One Unknown Probability Exceeds Another in View of Evidence of Two Samples'. In: *Biometrika* 25.3-4 (1933), pp. 285–294. DOI: `10.1093/biomet/25.3-4.285`. URL: `https://doi.org/10.1093/biomet/25.3-4.285`.

[3] Jaya Kawale and Elliot Chow. 'A Multi-Armed Bandit Framework for Recommendations at Netflix'. Data Council. 2018. URL: `https://www.datacouncil.ai/talks/a-multi-armed-bandit-framework-for-recommendations-at-netflix`.

[4] Daniel N. Hill et al. 'An Efficient Bandit Algorithm for Realtime Multivariate Optimization'. In: *Proceedings of the 23rd ACM SIGKDD International Conference on Knowledge Discovery and Data Mining*. KDD '17: The 23rd ACM SIGKDD International Conference on Knowledge Discovery and Data Mining. Halifax NS Canada: ACM, 2017, pp. 1813–1821. ISBN: 978-1-4503-4887-4. DOI: `10.1145/3097983.3098184`. URL: `https://dl.acm.org/doi/10.1145/3097983.3098184`.

[5] Sam Daulton. 'Facebook Talk at the Netflix ML Platform Meetup (Part 3)'. Machine Learning Platform (Los Gatos). 2019. URL: `https://youtu.be/A-JJvYaBPUU`.

[6] Arjun Sharma. *Using a Multi-Armed Bandit with Thompson Sampling to Identify Responsive Dashers*. DoorDash Engineering Blog. 2022. URL: `https://doordash.engineering/2022/03/15/using-a-multi-armed-bandit-with-thompson-sampling-to-identify-responsive-dashers/`.

[7] Tor Lattimore and Csaba Szepesvári. *Bandit Algorithms*. 1st ed. Cambridge University Press, 2020. ISBN: 978-1-108-57140-1 978-1-108-48682-8. DOI: `10.1017/9781108571401`. URL: `https://www.cambridge.org/core/product/identifier/9781108571401/type/book`.

[8] Aleksandrs Slivkins. 'Introduction to Multi-Armed Bandits'. In: *Foundations and Trends® in Machine Learning* 12.1-2 (2019), pp. 1–286. DOI: `10.1561/2200000068`. URL: `http://www.nowpublishers.com/article/Details/MAL-068`.

[9] T.L Lai and Herbert Robbins. 'Asymptotically Efficient Adaptive Allocation Rules'. In: *Advances in Applied Mathematics* 6.1 (1985), pp. 4–22. DOI: `10.1016/0196-8858(85)90002-8`. URL: `https://linkinghub.elsevier.com/retrieve/pii/0196885885900028`.

[10] Peter Auer et al. 'The Nonstochastic Multiarmed Bandit Problem'. In: *SIAM Journal on Computing* 32.1 (2002), pp. 48–77. DOI: `10.1137/S0097539701398375`. URL: `http://epubs.siam.org/doi/10.1137/S0097539701398375`.

[11] Pierre Ménard and Aurélien Garivier. 'A Minimax and Asymptotically Optimal Algorithm for Stochastic Bandits'. Version 2. In: (2017). DOI: `10.48550/ARXIV.1702.07211`. URL: `https://arxiv.org/abs/1702.07211`.

[12] Tianyuan Jin et al. 'MOTS: Minimax Optimal Thompson Sampling'. Version 3. In: (2020). DOI: `10.48550/ARXIV.2003.01803`. URL: `https://arxiv.org/abs/2003.01803`.

[13] Peter Auer, Nicolò Cesa-Bianchi and Paul Fischer. 'Finite-Time Analysis of the Multiarmed Bandit Problem'. In: *Machine Learning* 47.2 (2002), pp. 235–256. DOI: `10.1023/A:1013689704352`. URL: `https://doi.org/10.1023/A:1013689704352`.

[14] Sébastien Bubeck. 'Regret Analysis of Stochastic and Nonstochastic Multi-armed Bandit Problems'. In: *Foundations and Trends® in Machine Learning* 5.1 (2012), pp. 1–122. DOI: `10.1561/2200000024`. URL: `http://www.nowpublishers.com/article/Details/MAL-024`.

[15] Jean-Yves Audibert and Sëbastien Bubeck. 'Minimax Policies for Adversarial and Stochastic Bandits'. In: *Colt* 7 (2009), pp. 217–226.

[16] Jean-Yves Audibert, Rémi Munos and Csaba Szepesvári. 'Exploration–Exploitation Tradeoff Using Variance Estimates in Multi-Armed Bandits'. In: *Theoretical Computer Science* 410.19 (2009), pp. 1876–1902. DOI: `10.1016/j.tcs.2009.01.016`. URL: `https://linkinghub.elsevier.com/retrieve/pii/S030439750900067X`.

[17] Odalric-Ambrym Maillard, Rémi Munos and Gilles Stoltz. 'A Finite-Time Analysis of Multi-armed Bandits Problems with Kullback-Leibler Divergences'. Version 1. In: (2011). DOI: `10.48550/ARXIV.1105.5820`. URL: `https://arxiv.org/abs/1105.5820`.

[18] Emilie Kaufmann, Nathaniel Korda and Rémi Munos. 'Thompson Sampling: An Asymptotically Optimal Finite-Time Analysis'. In: *Algorithmic Learning Theory*. Ed. by Nader H. Bshouty et al. Red. by David Hutchison et al. Vol. 7568. Lecture Notes in Computer Science. Berlin, Heidelberg: Springer Berlin Heidelberg, 2012, pp. 199–213. ISBN: 978-3-642-34105-2 978-3-642-34106-9. DOI: `10.1007/978-3-642-34106-9_18`. URL: `http://link.springer.com/10.1007/978-3-642-34106-9_18`.

[19] Shipra Agrawal and Navin Goyal. 'Further Optimal Regret Bounds for Thompson Sampling'. In: *Proceedings of the Sixteenth International Conference on Artificial Intelligence and Statistics*. Artificial Intelligence and Statistics. PMLR, 2013, pp. 99–107. URL: `https://proceedings.mlr.press/v31/agrawal13a.html`.

[20] Shipra Agrawal and Navin Goyal. 'Near-Optimal Regret Bounds for Thompson Sampling'. In: *Journal of the ACM* 64.5 (2017), 30:1–30:24. DOI: `10.1145/3088510`. URL: `https://doi.org/10.1145/3088510`.

[21] Junya Honda and Akimichi Takemura. 'Optimality of Thompson Sampling for Gaussian Bandits Depends on Priors'. In: *Proceedings of the Seventeenth International Conference on Artificial Intelligence and Statistics*. Vol. 33. Reykjavik, Iceland}: PMLR, 2014, pp. 375–383. arXiv: `1311.1894 [math, stat]`. URL: `http://proceedings.mlr.press/v33/honda14.pdf`.

[22] Peter Auer et al. 'Gambling in a rigged casino: the adversarial multi-armed bandit problem'. In: *Annual Symposium on Foundations of Computer Science - Proceedings*. Proceedings of the 1995 IEEE 36th Annual Symposium on Foundations of Computer Science. 1995, pp. 322–331. URL: `https://collaborate.princeton.edu/en/publications/gambling-in-a-rigged-casino-the-adversarial-multi-armed-bandit-pr`.

[23] Lilian Besson and Emilie Kaufmann. 'What Doubling Tricks Can and Can't Do for Multi-Armed Bandits'. Version 1. In: (2018). DOI: 10.48550/ARXIV.1803.06971. URL: https://arxiv.org/abs/1803.06971.

[24] Michael A. Nielsen and Isaac L. Chuang. *Quantum Computation and Quantum Information: 10th Anniversary Edition*. 1st ed. Cambridge University Press, 2012. ISBN: 978-0-511-97666-7. DOI: 10.1017/CBO9780511976667. URL: https://www.cambridge.org/core/product/identifier/9780511976667/type/book.

[25] Amira Abbas et al. *Learn Quantum Computation Using Qiskit*. 2020. URL: https://qiskit.org/textbook/.

[26] Smite Meister. *Bloch sphere*. 2009. URL: https://upload.wikimedia.org/wikipedia/commons/6/6b/Bloch_sphere.svg.

[27] Giacomo Torlai et al. 'Precise Measurement of Quantum Observables with Neural-Network Estimators'. In: *Physical Review Research* 2.2 (2020), p. 022060. DOI: 10.1103/PhysRevResearch.2.022060. URL: https://link.aps.org/doi/10.1103/PhysRevResearch.2.022060.

[28] Danial Dervovic et al. 'Quantum Linear Systems Algorithms: A Primer'. 2018. DOI: 10.48550/ARXIV.1802.08227. arXiv: 1802.08227 [quant-ph]. URL: https://arxiv.org/abs/1802.08227.

[29] Scott Aaronson. 'Read the Fine Print'. In: *Nature Physics* 11.4 (2015), pp. 291–293. DOI: 10.1038/nphys3272. URL: http://www.nature.com/articles/nphys3272.

[30] Lov K. Grover. 'A Fast Quantum Mechanical Algorithm for Database Search'. In: *Proceedings of the Twenty-Eighth Annual ACM Symposium on Theory of Computing*. Philadelphia, Pennsylvania, United States of America: ACM Press, 1996, pp. 212–219. ISBN: 978-0-89791-785-8. DOI: 10.1145/237814.237866. URL: http://portal.acm.org/citation.cfm?doid=237814.237866.

[31] Christof Zalka. 'Grover's Quantum Searching Algorithm Is Optimal'. In: *Physical Review A* 60.4 (1999), pp. 2746–2751. DOI: 10.1103/PhysRevA.60.2746. URL: https://link.aps.org/doi/10.1103/PhysRevA.60.2746.

[32] Gilles Brassard et al. 'Quantum Amplitude Amplification and Estimation'. In: *Contemporary Mathematics*. Ed. by Samuel J. Lomonaco and Howard E. Brandt. Vol. 305. Providence, Rhode Island: American Mathematical Society, 2002, pp. 53–74. ISBN: 978-0-8218-2140-4 978-0-8218-7895-8. DOI: `10.1090/conm/305/05215`. URL: `http://www.ams.org/conm/305/`.

[33] Ashley Montanaro. 'Quantum Speedup of Monte Carlo Methods'. In: *Proceedings of the Royal Society A: Mathematical, Physical and Engineering Sciences* 471.2181 (2015), p. 20150301. DOI: `10.1098/rspa.2015.0301`. URL: `https://royalsocietypublishing.org/doi/10.1098/rspa.2015.0301`.

[34] Yohichi Suzuki et al. 'Amplitude Estimation without Phase Estimation'. In: *Quantum Information Processing* 19.2 (2020), p. 75. DOI: `10.1007/s11128-019-2565-2`. arXiv: `1904.10246 [quant-ph]`. URL: `http://arxiv.org/abs/1904.10246`.

[35] Kouhei Nakaji. 'Faster Amplitude Estimation'. In: *Quantum Information and Computation* 20 (2020), pp. 1109–1123. DOI: `10.26421/QIC20.13-14-2`.

[36] Dmitry Grinko et al. 'Iterative Quantum Amplitude Estimation'. In: *npj Quantum Information* 7.1 (2021), p. 52. DOI: `10.1038/s41534-021-00379-1`. arXiv: `1912.05559 [quant-ph]`. URL: `http://arxiv.org/abs/1912.05559`.

[37] David Ceperley and Berni Alder. 'Quantum Monte Carlo'. In: *Science* 231.4738 (1986), pp. 555–560. DOI: `10.1126/science.231.4738.555`. URL: `https://www.science.org/doi/10.1126/science.231.4738.555`.

[38] Brian M. Austin, Dmitry Yu. Zubarev and William A. Lester. 'Quantum Monte Carlo and Related Approaches'. In: *Chemical Reviews* 112.1 (2012), pp. 263–288. DOI: `10.1021/cr2001564`. URL: `https://pubs.acs.org/doi/10.1021/cr2001564`.

[39] J. E. Gubernatis, N. Kawashima and P. Werner. *Quantum Monte Carlo Methods: Algorithms for Lattice Models*. Cambridge: Cambridge University Press, 2016. 488 pp. ISBN: 978-1-107-00642-3.

[40] Paul Dagum et al. 'An Optimal Algorithm for Monte Carlo Estimation'. In: *SIAM Journal on Computing* 29.5 (2000), pp. 1484–1496. DOI: `10.1137/S0097539797315306`. URL: `https://epubs.siam.org/doi/10.1137/S0097539797315306`.

[41] Zongqi Wan et al. 'Quantum Multi-Armed Bandits and Stochastic Linear Bandits Enjoy Logarithmic Regrets'. Version 1. In: (2022). DOI: 10.48550/ARXIV.2205.14988. URL: https://arxiv.org/abs/2205.14988.

[42] Balthazar Casalé et al. 'Quantum Bandits'. In: *Quantum Machine Intelligence* 2.1 (2020), p. 11. DOI: 10.1007/s42484-020-00024-8. URL: https://link.springer.com/10.1007/s42484-020-00024-8.

[43] Daochen Wang et al. 'Quantum Exploration Algorithms for Multi-Armed Bandits'. In: *Proceedings of the AAAI Conference on Artificial Intelligence* 35.11 (11 2021), pp. 10102–10110. DOI: 10.1609/aaai.v35i11.17212. URL: https://ojs.aaai.org/index.php/AAAI/article/view/17212.